WATER RESOURCES RESEARCH, VOL. 28, NO. 4, PAGES 1179–1186, APRIL 1992

Modification of the Kinematic Wave–Philip Infiltration Overland Flow Model

CHARLES H. LUCE

USDA Forest Service Intermountain Forest and Range Experiment Station, Moscow, Idaho

TERRANCE W. CUNDY

University of Washington, Seattle

In previous work a solution was developed for the kinematic wave overland flow equation with rainfall excess given by Philip's infiltration equation. Subsequent application of this solution to field data from small plots revealed the need for an improved model. The principal requirement is the incorporation of depression storage into the rising limb calculation. A second requirement is a more precise approximation of the water surface profile at the end of rainfall. This improves the falling limb calculations. This paper shows the solutions obtained by incorporating these improvements and demonstrates their effects on predicted hydrographs and water surface profiles.

REVIEW

Cundy and Tento [1985] developed a solution to the kinematic wave overland flow equation with rainfall excess given by *Philip*'s [1969] infiltration equation. *Luce* [1990] applied the kinematic wave–Philip (KWP) model to 1 m by 1 m plots on freshly graded forest road surfaces to identify soil and hydraulic parameters. Figure 1 shows a field-measured and a fitted hydrograph illustrating the limitations of the KWP model. The fitted roughness is an order of magnitude higher than the range given by *Woolhiser* [1975] for similar surfaces. This results in overestimation of the falling limb. Furthermore, the model could not reproduce the observed lag between the start of rainfall and the start of runoff. These same problems were encountered in fitting other plots.

The most likely process to produce the observed delay in runoff is depression storage, which is not included in the model. On artificial plots of sand grains glued to Plexiglas, *Katz* [1990] measured depression storage values of approximately 0.067 cm. As will be demonstrated later, even this small amount of depression storage significantly affects the hydrograph and fitted values of roughness.

In addition, the initial condition for the falling limb calculations was found to contribute to the overestimate of roughness. It was modified as suggested by *Dunne and Dietrich* [1980].

This paper shows the solutions obtained by incorporating these changes and demonstrates their effects on predicted hydrographs and water surface profiles.

BACKGROUND

The equation used here for flow over a plane under the kinematic wave approximation is

$$\alpha\beta h^{\beta-1}\frac{\partial h}{\partial x}+\frac{\partial h}{\partial t}=i-f(t) \tag{1}$$

Copyright 1992 by the American Geophysical Union.

Paper number: 91WR03131.
0043-1397/92/91WR-03131$02.00

where h is the flow depth (L), x is the distance downslope (L), t is time (T), i is a constant rainfall rate (L/T), $f(t)$ is the infiltration rate (L/T), and α and β describe the stage discharge relationship defined below. *Philip* [1969] described infiltration rate in the form

$$f(t)=A+B[t-(t_p-t_s)]^{-1/2} \tag{2}$$

where $f(t)$ is the infiltration rate t (L/T), A is the conductivity of the soil (L/T), and B is the sorptivity of the soil at the initial soil moisture content ($L/T^{1/2}$). The factor $t_p - t_s$ is a time correction composed of the actual time to ponding (t_p) and the time when $f(t) = i$ under continuously ponded conditions (t_s) [*Cundy and Tento*, 1985].

The parameters α and β define the stage-discharge relationship. The discharge per unit width is given by

$$q=\alpha h^{\beta} \tag{3}$$

Calculations for laminar and turbulent flow differ only in minor details; calculations for laminar flow are presented here, and equations for turbulent flow are presented in the appendix. For laminar flow,

$$\alpha=\frac{gS}{k\nu} \tag{4}$$

$$\beta=3 \tag{5}$$

where g is gravity (L/T^2), S is the bed slope (L/L), ν is the kinematic viscosity (L^2/T), and k is a roughness coefficient.

DEVELOPMENT

Referring to Figure 2, a rainfall event in the x, t plane can be described as follows. At the start of rainfall $t = 0$. For a period of time, $0 < t < t_p$, all the rainfall infiltrates. At t_p surface saturation occurs and rainfall excess begins to fill depression storage. For some time after t_p, call it t_n, it can be assumed that all rainfall excess is used to fill depression storage. For $t > t_n$, overland flow occurs. Following the end of rainfall, $t > t_r$, infiltration and overland flow continue.

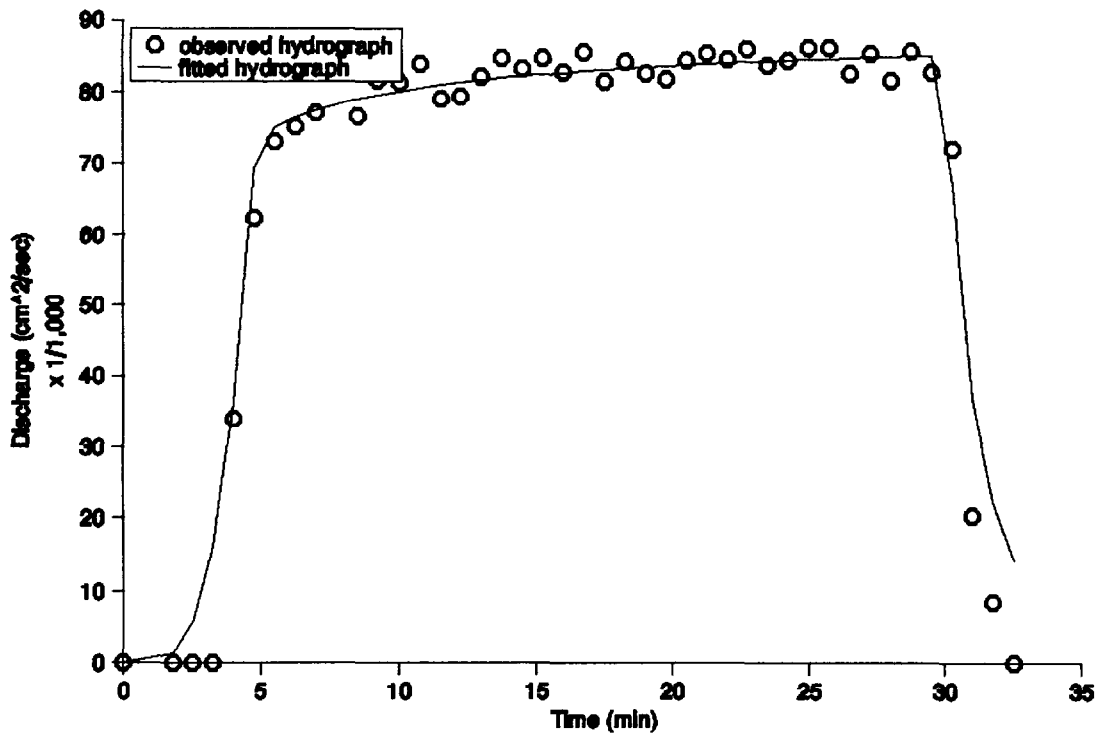

Fig. 1. Best fit of field hydrograph from 1 m by 1 m plot on freshly graded forest road using kinematic wave–Philip model. Slope is 6.5%. Median surface diameter is 3 mm. Rainfall was applied at 3.47 cm/h for 30 min. Fitted hydraulic conductivity, A = 0.156 cm/h. Fitted sorptivity B = 0.155 cm/h$^{1/2}$. Fitted roughness, k = 4000. Reynolds number is approximately 8.

The time at which each point on the surface dries is given by t_d.

Using the method of characteristics as done by *Cundy and Tento* [1985], where τ is used to describe the initial point of the characteristic along the x, t axes, and s is used to describe the time along each characteristic, the solution to (1) is given below in three steps: (1) infiltration and depression storage processes before runoff begins, (2) the rising stage of the hydrograph, and (3) the falling stage of the hydrograph.

Infiltration and Depression Storage

As stated above, infiltration is calculated using *Philip*'s [1969] equation adjusted for a constant intensity rainfall (2). In this analysis the process of depression storage is included between the time of ponding and the time runoff begins. If the depth of depression storage (h_n) is known, then the time at which it is filled (t_n) is given by

$$h_n = \int_{t_p}^{t_n} i - f(t)\, dt \tag{6}$$

With $f(t)$ described by (2) this gives

$$h_n = (i - A)(t_n - t_p) - 2B(t_n - t_p + t_s)^{1/2} + 2Bt_s^{1/2} \tag{7}$$

where t_n must be evaluated numerically. The time runoff begins is given by t_n.

Rising Stage

For laminar flow conditions, (1) becomes

$$3\alpha h^2 \frac{\partial h}{\partial x} + \frac{\partial h}{\partial t} = i - A - B(t - t_p + t_s)^{-1/2} \tag{8}$$

The initial condition for (8) becomes $h(x, t_n) = 0$ and the solution to (8) is

$$t(s, \tau) = s + t_n \qquad \tau \le 0 \tag{9a}$$

$$t(s, \tau) = s + \tau + t_n \qquad \tau > 0 \tag{9b}$$

$$h(s, \tau) = (i - A)s - 2B(s + t_m)^{1/2} + 2Bt_m^{1/2} \qquad \tau \le 0 \tag{10a}$$

$$h(s, \tau) = (i - A)s - 2B(s + \tau + t_m)^{1/2} + 2B(\tau + t_m)^{1/2} \qquad \tau > 0 \tag{10b}$$

$$\begin{aligned} x(s, \tau) = {} & \alpha(i - A)^2 s^3 + 1.6\alpha B(i - A)(2t_m - 3s)(s + t_m)^{3/2} \\ & + 6\alpha B(i - A)t_m^{1/2}s^2 + 6\alpha B^2 s^2 + 24\alpha B^2 t_m s \\ & - 16\alpha B^2 t_m^{1/2}(s + t_m)^{3/2} + 16\alpha B^2 t_m^2 \\ & - 3.2\alpha B(i - A)t_m^{5/2} - \tau \qquad \tau \le 0 \end{aligned} \tag{11a}$$

$$\begin{aligned} x(s, \tau) = {} & \alpha(i - A)^2 s^3 + 1.6\alpha B(i - A)(2\tau + 2t_m - 3s) \\ & \cdot (s + \tau + t_m)^{3/2} + 6\alpha B(i - A)(\tau + t_m)^{1/2}s^2 \\ & + 6\alpha B^2 s^2 + 24\alpha B^2(\tau + t_m)s - 16\alpha B^2(\tau + t_m)^{1/2} \\ & \cdot (s + \tau + t_m)^{3/2} + 16\alpha B^2(\tau + t_m)^2 \\ & - 3.2\alpha B(i - A)(\tau + t_m)^{5/2} \qquad \tau > 0 \end{aligned} \tag{11b}$$

where $t_m = t_n - t_p + t_s$. For the case $h_n = 0$, and thus $t_n = 0$, these equations reduce to those of *Cundy and Tento* [1985].

The solution procedures for determining hydrographs at

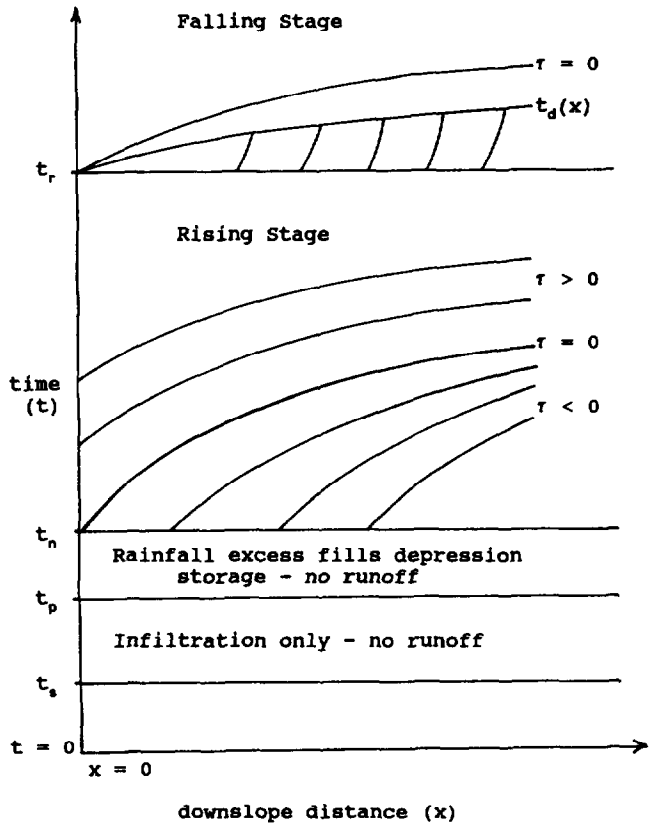

Fig. 2. Rainfall event in the x, t plane.

fixed slope positions, and water surface profiles at fixed times are identical to those of *Cundy and Tento* [1985].

Falling Stage

The falling stage begins when $t = t_r$, the time when rainfall ends; the equation to solve is

$$3\alpha h^2 \frac{\partial h}{\partial x} + \frac{\partial h}{\partial t} = -A - B(t - t_p + t_s)^{-1/2} \qquad (12)$$

The initial conditions for this equation are the x, $t = t_r$ axis (Figure 2) along which $h(x, t)$ must be known. For $-\tau > x'$, where x' is the position of the $\tau = 0$ characteristic at $t = t_r$, the water surface profile is flat and is a function of t_r only:

$$h(-\tau > x', t_r) = (i - A)(t_r - t_n) - 2B(t_r - t_p + t_s)^{1/2} + 2Bt_m^{1/2} \qquad (13)$$

For $-\tau < x'$ the flow is unsteady-nonuniform and a closed form solution cannot be found, so the initial condition is modeled by $h = \varepsilon x^n$, where h is water depth (L), x is distance downslope (L), and ε is a fitted parameter. Then ε can be fit by least squares using h, x pairs with $x < x'$, or can be calculated by rearranging the equation to $\varepsilon = h/x^n$ and using $h = h(x = x', t = t_r)$, $x = x'$. *Cundy and Tento* [1985] used $n = \frac{1}{2}$. *Luce* [1990] used *Dunne and Dietrich*'s [1980] suggestion to estimate the water surface profile using $n = 1/\beta$, where $\beta = 3$ for laminar flows and $\beta = \frac{3}{2}$ for turbulent flows, and found better fits (Figure 3). The effects of changing n from 1/2 to $1/\beta$ on the hydrograph and water surface

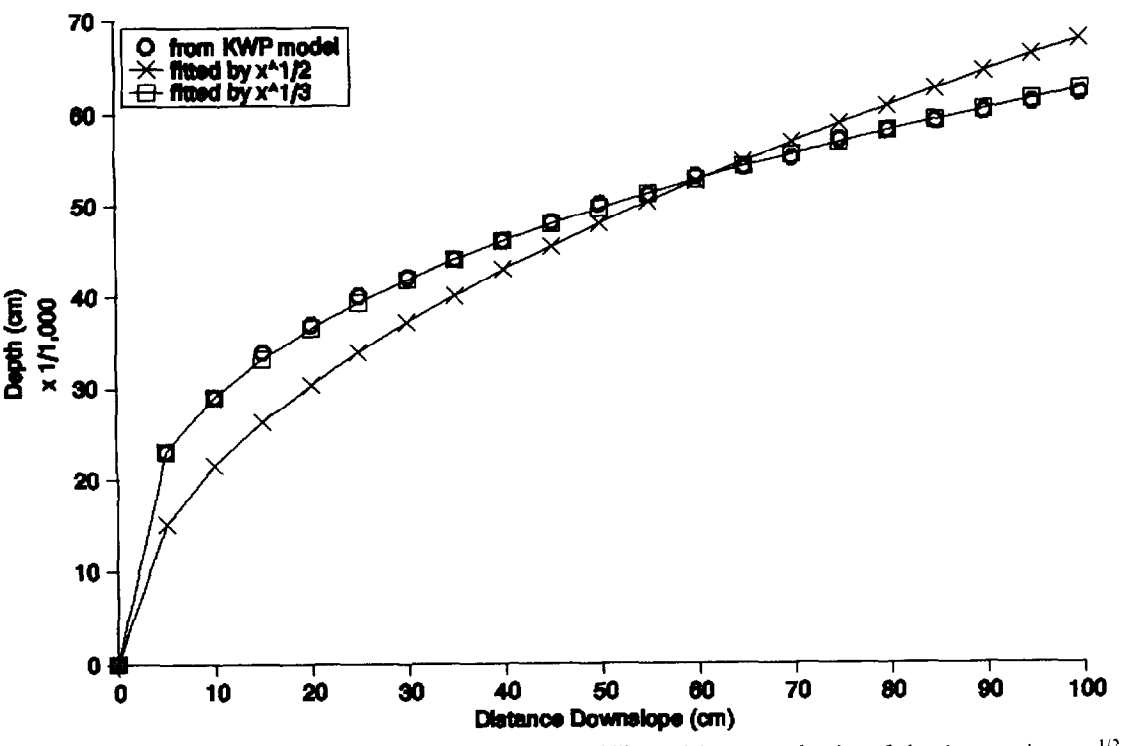

Fig. 3. Water surface profile calculated by kinematic wave–Philip model compared to best fit by the equations $\varepsilon x^{1/2}$ and $\varepsilon x^{1/3}$.

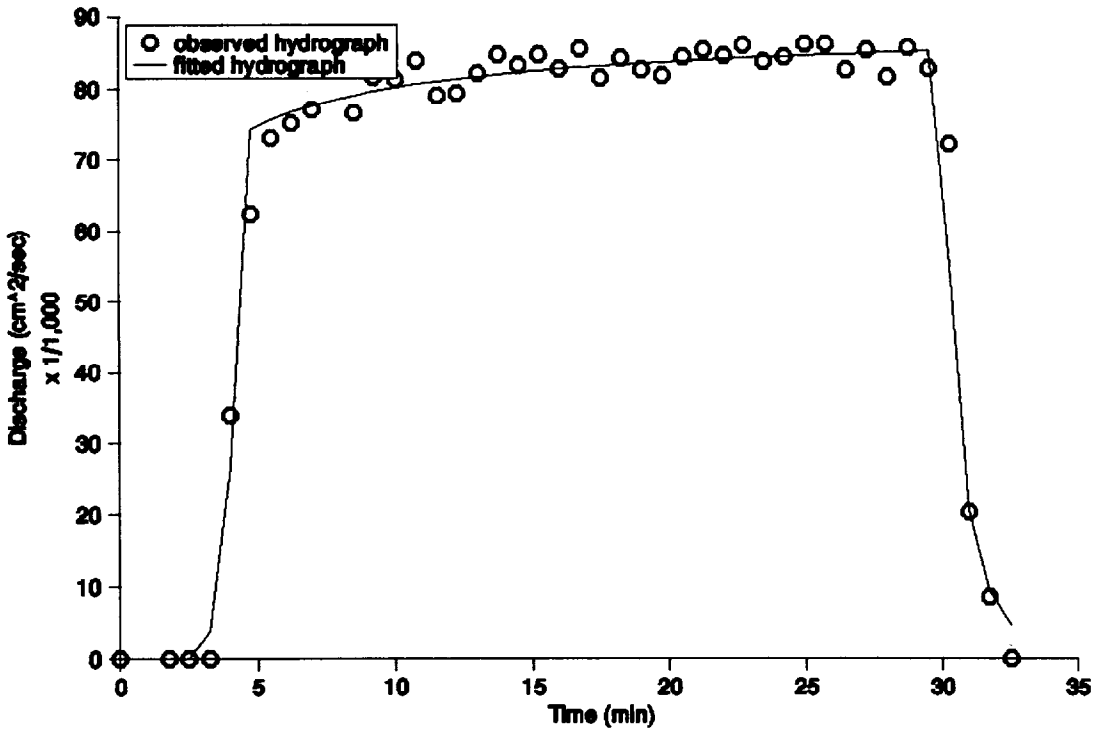

Fig. 4. Best fit of hydrograph displayed in Figure 1 by kinematic wave–Philip model with depression storage. Fitted depression storage, h_n = 0.07 cm. Fitted hydraulic conductivity, A = 0.174 cm/h. Fitted sorptivity, B = 0.162 cm/h$^{1/2}$. Fitted roughness, k = 616.

profiles are shown later. In the case of steady infiltration rate, $B = 0$, $n = 1/\beta$ is exact. For $B > 0$, $n = 1/\beta$ is nearly exact, and ε depends on rainfall duration.

The solution to (12) is given by

$$t(s, \tau) = s + t_r \tag{14}$$

$$h(s, \tau) = -As - 2B(s + r)^{1/2} + (i - A)(t_r - t_p) + 2Bt_s^{1/2} \qquad -\tau > x' \tag{15a}$$

$$h(s, \tau) = -As - 2B(s + r)^{1/2} + \varepsilon(-\tau)^{1/\beta} + 2Br^{1/2} \qquad -\tau \le x' \tag{15b}$$

$$\begin{aligned} x(s, \tau) = {} & \alpha A^2 s^3 - 1.6\alpha AB(2r - 3s)(s + r)^{3/2} - 3\alpha A(i - A) \\ & \cdot (t_r - t_p)s^2 - 6\alpha ABt_s^{1/2}s^2 + 6\alpha B^2 s^2 \\ & + 12\alpha B^2 t_r s - 12\alpha B^2 t_p s + 24\alpha B^2 t_s s \\ & - 8\alpha B(i - A)(t_r - t_p)(s + r)^{3/2} \\ & - 16\alpha B^2 t_s^{1/2}(s + r)^{3/2} + 3\alpha(i - A)^2(t_r - t_p)^2 s \\ & + 12\alpha Bt_s^{1/2}(i - A)(t_r - t_p)s + 3.2\alpha ABr^{5/2} \\ & + 8\alpha B(i - A)(t_r - t_p)r^{3/2} \\ & + 16\alpha B^2 t_s^{1/2} r^{3/2} - \tau \qquad -\tau > x' \end{aligned} \tag{16a}$$

$$\begin{aligned} x(s, \tau) = {} & \alpha A^2 s^3 - 1.6\alpha AB(2r - 3s)(s + r)^{3/2} \\ & - 3\alpha A\varepsilon(-\tau)^{1/3}s^2 - 6\alpha ABr^{1/2}s^2 + 6\alpha B^2 s^2 \\ & + 24\alpha B^2(t_r - t_p + t_s)s - 8\alpha B\varepsilon(-\tau)^{1/3}(s + r)^{3/2} \\ & - 16\alpha B^2 r^{1/2}(s + r)^{3/2} - 3\alpha\varepsilon^2(-\tau)^{2/3}s \\ & + 12\alpha B\varepsilon(-\tau)^{1/3}r^{1/2}s + 3.2\alpha ABr^{5/2} \\ & + 8\alpha B\varepsilon(-\tau)^{1/3}r^{3/2} \\ & + 16\alpha B^2 r^2 - \tau \qquad 0 \le -\tau \le x' \end{aligned} \tag{16b}$$

where $r = t_r - t_p + t_s$. The falling stage solution procedures for hydrographs and water surface profiles given by *Cundy and Tento* [1985] again apply fully.

Application to Field Data

Figure 4 shows the hydrograph of Figure 1 modeled using the modifications presented above. A depression storage value of 0.07 cm was used, which is consistent with the

TABLE 1. Hillslope and Rainfall Attributes: Infiltration and Hydraulic Parameters for the Example Problem

Parameter	Value
i	4 cm/h
A	0.5 cm/h
B	1.5 cm/h$^{1/2}$
S	0.05
k	100
h_n	0.05 cm
α	353,160 cm^{-1} hr^{-1}
β	3
t_s	0.184 h
t_p	0.344 h
t_n	0.461 h

The parameters reflect a very dry, bare, coarse sand surface.

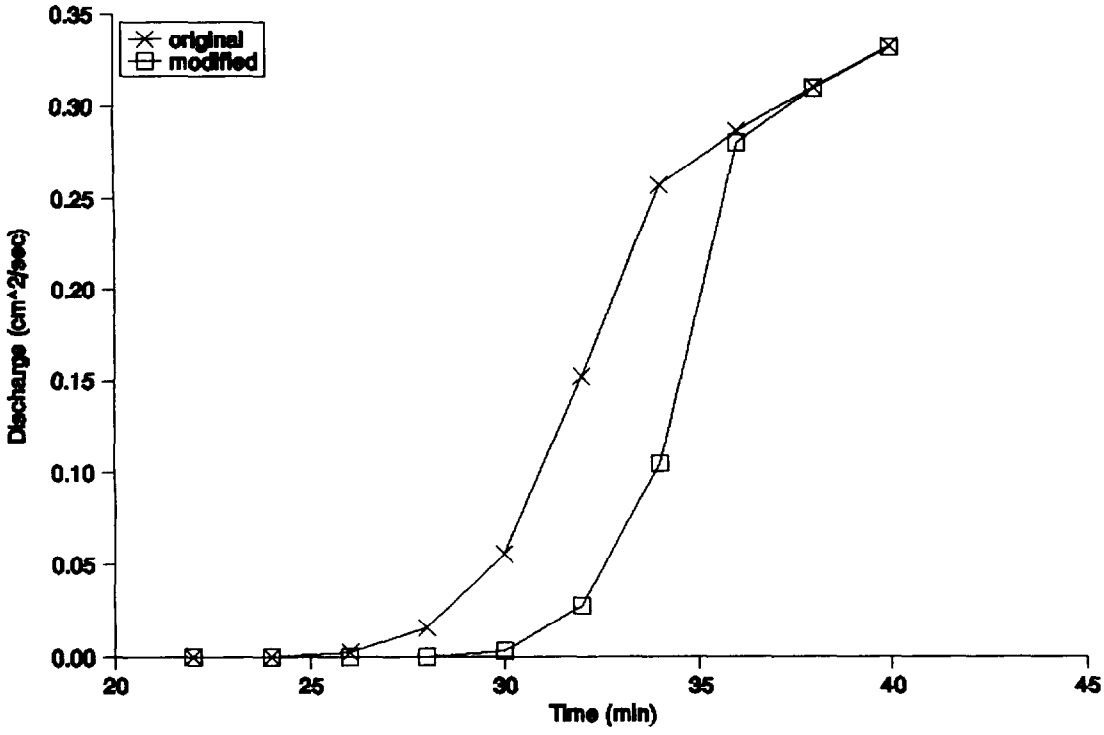

Fig. 5. Rising stage hydrographs at x = 900 cm from the original and modified model.

values determined by *Katz* [1990]. The values of A, B and k were determined using a grid-based search [*Luce*, 1990].

The first improvement is that the fitted k value is now 616, which is close to the range for similar surfaces of 90–400 listed by *Woolhiser* [1975]. This results in the second improvement, that the falling limb is no longer overpredicted.

The third improvement is that the observed delay in runoff is now reproduced. In Figure 1, runoff begins almost immediately, while in Figure 4, runoff is delayed for almost 2.5 min, which is consistent with the field observations.

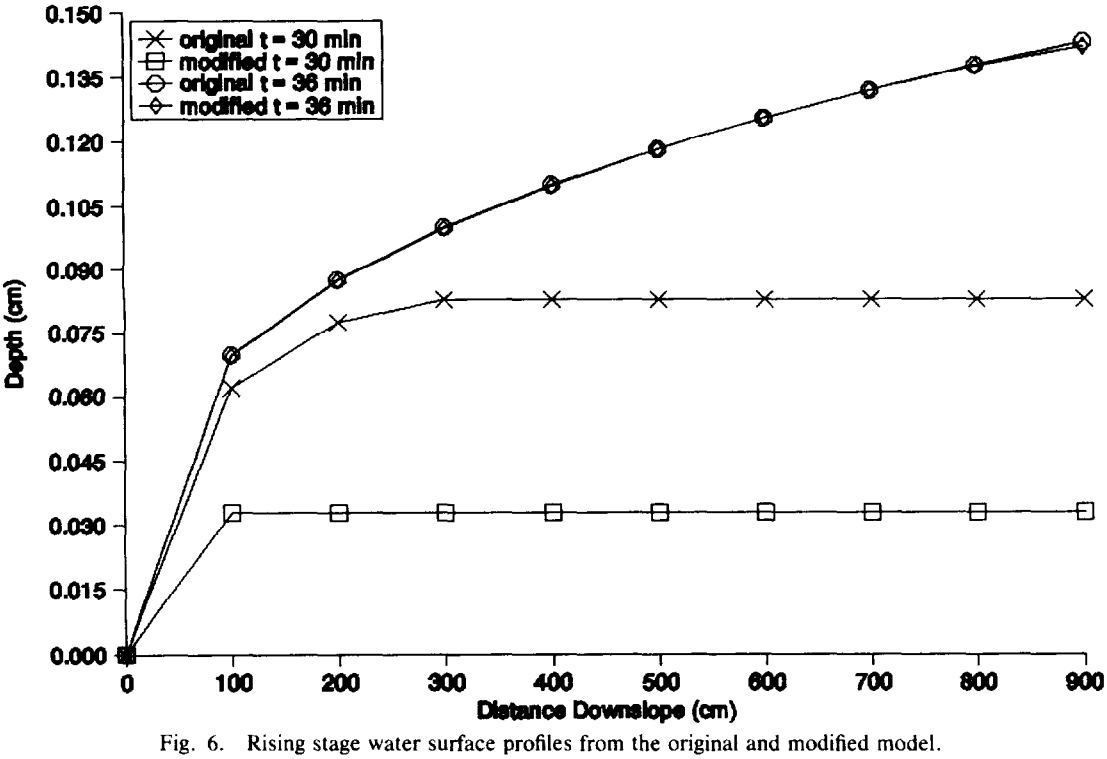

Fig. 6. Rising stage water surface profiles from the original and modified model.

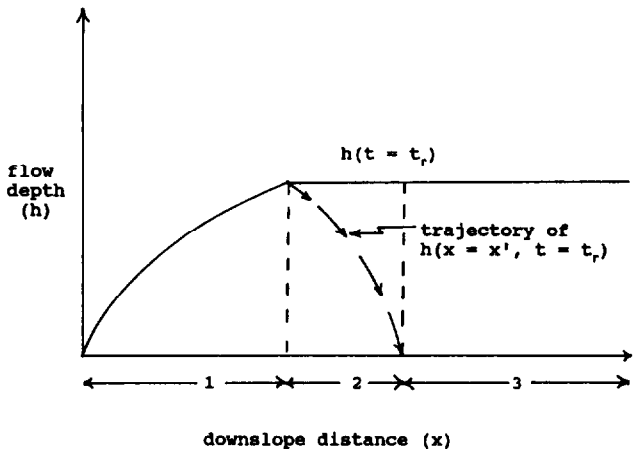

Fig. 7. Definition of three regions for the falling stage.

EXAMPLE PROBLEM

To further demonstrate the effects of the modifications to the model on hydrographs and water surface profiles, an example problem is given below. Table 1 contains the hillslope and rainfall attributes used, and the infiltration and hydraulic parameters calculated from these attributes.

Rising Stage Hydrograph at a Fixed Point

The rising limbs of the hydrographs for the two models for $x = 900$ cm are shown in Figure 5. With depression storage the hydrograph starts rising later and steeper. The steeper rise is due to the greater rainfall excess rate when flow begins. After the $\tau = 0$ characteristic passes and the entire slope is contributing runoff, both hydrographs are identical.

Rising Stage Water Surface Profiles

Water surface profiles for the two models are shown in Figure 6. Again, with depression storage the profiles rise later, but after the $\tau = 0$ characteristic passes the profiles coincide identically.

Falling Stage Hydrograph at a Fixed Point

Recalling from the development above that the falling stage of the model was improved through a better approximation of the water surface profile at $t = t_r$ and $x < x'$, the effect on a hydrograph at a fixed point will only be seen if that point lies in region 1 or 2 as defined by *Cundy and Tento* [1985, Figure 7], reproduced here as Figure 7.

Figure 8 shows the falling stage hydrographs for both models for $x = 900$ cm. The square root approximation used by *Cundy and Tento* [1985] yields discharge estimates that are lower than those computed from the cube root approximation.

Falling Stage Water Surface Profiles

Figure 9 shows falling stage water surface profiles for both models. Again, these show that for the unsteady-nonuniform part of the profile, the square root approximation used by *Cundy and Tento* [1985] results in depth estimates that are too low. This further leads to underestimation of drying times along the slope.

CONCLUSION

Modifications of the kinematic wave–Philip model of *Cundy and Tento* [1985] have been presented. These are (1) the inclusion of depression storage, and (2) an improved

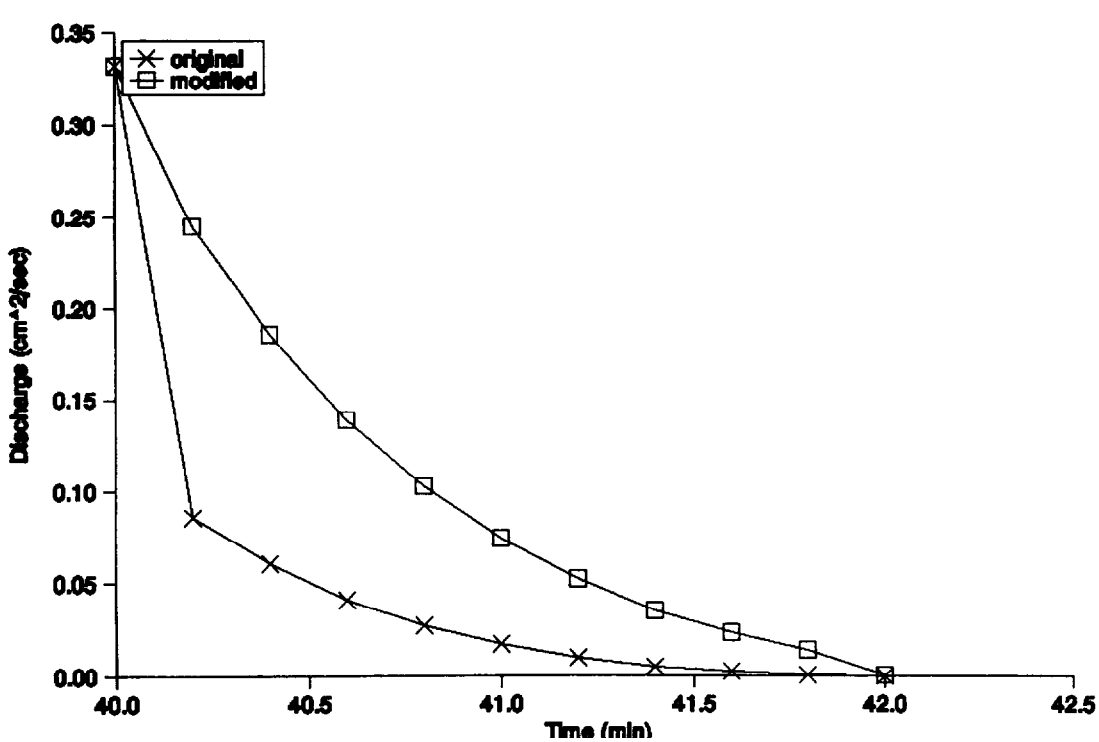

Fig. 8. Falling stage hydrographs at $x = 900$ cm from the original and modified model.

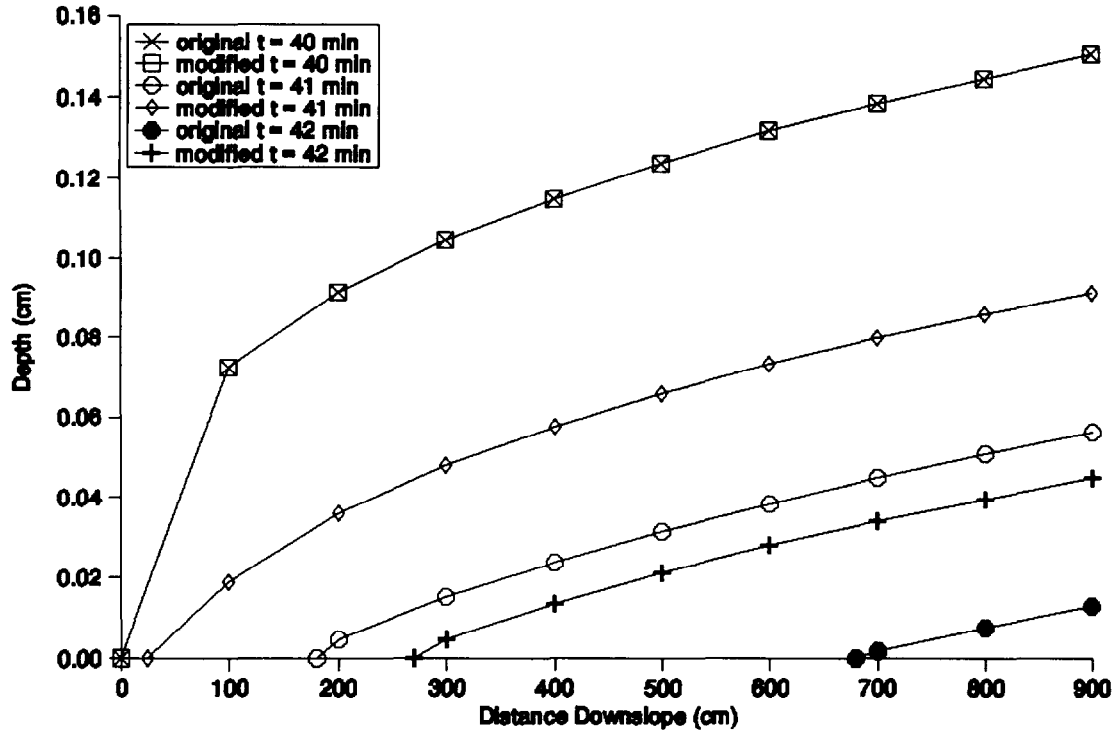

Fig. 9. Falling stage water surface profiles from the original and modified model.

approximation of the unsteady-nonuniform part of the water storage profile at the end of rainfall.

These modifications give significant changes in hydrographs and water surface profiles predicted by the model. The most obvious changes result from depression storage effects on the initiation of overland flow.

As demonstrated on the field hydrograph, the improvement in fitting parameters is significant, in particular for estimates of roughness.

APPENDIX

Solutions for $x(s, \tau)$ are given below for the turbulent flow case. The solutions for $t(s, \tau)$ and $h(s, \tau)$ are identical to the laminar flow case.

For turbulent flow

$$\alpha = CS^{1/2} \tag{A1}$$

$$\beta = 3/2 \tag{A2}$$

where C is the Chezy coefficient.

Rising Stage

$$\begin{aligned} x(s, \tau) = {} & \alpha(i - A)^{1/2}(s + t_m)^{3/2} - 1.5\alpha B(s + t_m) \\ & \cdot (i - A)^{-1/2} - \alpha(i - A)^{1/2} t_m^{3/2} \\ & + 1.5\alpha B t_s (i - A)^{-1/2} - \tau \qquad \tau \le 0 \end{aligned} \tag{A3a}$$

$$\begin{aligned} x(u, \tau) = {} & \alpha U^{3/2}/c - 3\alpha b(2cu + b)U^{1/2}/(8c^2) \\ & - 3\alpha(4abc - b^3)/(16c^{5/2}) \\ & \cdot \log (2c^{1/2}U^{1/2} + 2cu + b) \\ & + 3\alpha(4abc - b^3)/(16c^{5/2}) \\ & \cdot \log [2c(\tau + t_m)^{1/2} + b] \quad \tau > 0 \end{aligned} \tag{A3b}$$

where

$$a = 2B(\tau + t_m)^{1/2} - (\tau + t_m)(i - A) \tag{A4}$$

$$b = -2B \tag{A5}$$

$$c = i - A \tag{A6}$$

$$u = (s + \tau + t_m)^{1/2} \tag{A7}$$

$$U = a + bu + cu^2 \tag{A8}$$

Falling Stage

$$\begin{aligned} x(u, \tau) = {} & \alpha U^{3/2}/c - 3\alpha b(2cu + b)U^{1/2}/(8c^2) \\ & - 3\alpha(4abc - b^3)/(16c^{5/2}) \\ & \cdot \log (2c^{1/2}U^{1/2} + 2cu + b) \\ & - \alpha V^{3/2}/c - 3\alpha b(2cv + b)V^{1/2}/(8c^2) \\ & - 3\alpha(4abc - b^3)/(16c^{5/2}) \\ & \cdot \log (2c^{1/2}V^{1/2} + 2cv + b) - \tau \qquad -\tau > x' \end{aligned} \tag{A9}$$

where

$$a = i(t_r - t_p) + 2Bt_m^{1/2} + At_m \tag{A10}$$

$$b = -2B \tag{A11}$$

$$c = -A \tag{A12}$$

$$u = (s + t_r - t_p + t_s)^{1/2} \tag{A13}$$

$$U = a + bu + cu^2 \tag{A14}$$

$$v = (t_r - t_p + t_s)^{1/2} \tag{A15}$$

$$V = a + bv + cv^2 \tag{A16}$$

The equation for $x(u, \tau)$ for $-\tau \leq x'$ is identical to (A9) with $a = \varepsilon(-\tau)^{2/3} + 2B(t_r - t_p + t_s)^{1/2} + A(t_r - t_p + t_s)$.

Acknowledgment. This research was supported by the U.S. Forest Service Intermountain Forest and Range Experiment Station under grant INT-90472-COA with the University of Washington.

REFERENCES

Cundy, T. W., and S. W. Tento, Solution to the kinematic wave approach to overland flow routing with rainfall excess given by Philip's equation, *Water Resour. Res.*, *21*(8), 1132–1140, 1985.

Dunne, T., and W. E. Dietrich, Experimental investigation of Horton overland flow on tropical hillslopes, 2, Hydraulic characteristics and hillslope hydrographs, *Z. Geomorphol. Suppl.*, *33*, 60–80, 1980.

Katz, D. M., The effects of surface roughness and rainfall impact on the hydraulics of overland flow, M.S. thesis, Univ. of Idaho, Moscow, 1990.

Luce, C. H., Analysis of infiltration and overland flow from small plots on forest roads, M.S. thesis, Univ. of Washington, Seattle, 1990.

Philip, J. R., *Theory of Infiltration*, *Adv. in Hydrosci.*, vol. 5, Academic, San Diego, Calif., 1969.

Woolhiser, D. A., Simulation of unsteady overland flow, in *Unsteady Flow in Open Channels*, edited by K. Mahmood and V. M. Yevjevich, pp. 485–508, Water Resources Publications, Fort Collins, Colo., 1975.

T. W. Cundy, College of Forest Resources, AR-10, University of Washington, Seattle, WA 98195.

C. H. Luce, USDA Forest Service Intermountain Forest and Range Experiment Station, 1221 South Main, Moscow, ID 83843.

(Received September 26, 1991;
revised December 11, 1991;
accepted December 16, 1991.)